JOURNAL OF MATERIALS SCIENCE **34** (1999) 957–966

Reactions between $La_{1-x}Ca_xMnO_3$ and CaO-stabilized ZrO_2

Part I *Powder mixtures*

S. FAALAND, M.-A. EINARSRUD, K. WIIK, T. GRANDE
Department of Inorganic Chemistry, Norwegian University of Science and Technology, 7034 Trondheim, Norway
E-mail: tor.grande@chembio.ntnu.no

The chemistry and microstructure of the interface between calcium substituted lanthanum manganite and cubic calcia stabilized zirconia have been studied. The aim was to investigate the chemical stability of these materials as a model system for, respectively, the cathode and the electrolyte in solid oxide fuel cells. The relative amounts and time dependence of the formation of secondary phases ($La_2Zr_2O_7$ and $CaZrO_3$) and inter-diffusion between the primary phases were observed to depend on temperature, partial pressure of oxygen, and composition of the manganite. 30 mole % Ca on La-site and A-site deficiency of the manganite were shown to stabilize the heterophase interface in air. Reducing conditions were shown to destabilize the primary phases and increase the rate of formation of secondary phases. Pore-coarsening with increasing amount of Ca in the manganite was the most striking feature in the time dependence of the microstructure. The present findings are discussed in relation to the thermodynamic and kinetic stability of the cathode/electrolyte interface of conventional solid oxide fuel cells consisting of yttria stabilized zirconia and strontium substituted lanthanum manganite. © *1999 Kluwer Academic Publishers*

1. Introduction

The study of heterophase solid state interfaces becomes increasingly important because of numerous applications requiring long-time stability of such interfaces. Solid oxide fuel cells (SOFC) and ceramic oxygen-permeating membranes are examples of systems possessing solid state interfaces between a perovskite-type oxide (ABO_3) and another ceramic material. In solid oxide fuel cells, lanthanum manganite-based oxides, e.g., $La_{1-x}Ca_xMnO_3$ (LCM) and $La_{1-x}Sr_xMnO_3$ (LSM), are promising materials as cathodes because of their high electrical conductivity and relatively good compatibility with cubic stabilized zirconia, which is the most common electrolyte. The reactivity of $La_{1-x}Ca_xMnO_3$ with yttria stabilized zirconia (YSZ) has been studied by several researchers [1–7]. The formation of secondary phases, such as $La_2Zr_2O_7$ (LZ) and $CaZrO_3$ (CZ), at the interface as well as interdiffusion of cations between the cell components will have a negative impact on the SOFC performance. A reaction mechanism has been proposed by Taimatsu *et al*. [6] for the formation of LZ at the YSZ/$La_{1-x}Ca_xMnO_3$ ($x = 0$, 0.1, 0.2) boundary, but no mechanism has so far been discussed for the calcia stabilized zirconia (CSZ)/LCM system. Yokokawa *et al*. [8] proposed that a high oxygen potential was needed for the formation of LZ at the YSZ/lanthanum manganite (LM) interface. However, the effect of the partial pressure of oxygen on the formation of secondary phases in the CSZ/LCM system has so far not been reported.

In this work we have studied a model system for the electrode/electrolyte interface consisting of LCM and CSZ. The thermodynamic driving force for the formation of secondary phases is reduced in this model by replacing yttria in zirconia with calcia. This substitution was performed in order to obtain a better understanding of the effect of different dopants on the stability of the electrode/electrolyte materials conventionally being used in SOFC (LSM and YSZ) [9]. In the present paper, which is the first in a series of two, reactions between LCM and CSZ have been investigated in compressed powder mixtures corresponding to a 1:1 mass ratio of LCM and CSZ. Hence, the interface area between the reactants has been maximized, and equilibrium phase composition is expected to be established fast relative to the phase composition at the conventional interface in SOFC. In a second paper, the corresponding reactions are studied by a different model using diffusion couples, a situation closer to the geometry of real fuel cells [10]. The aim of the present investigation is twofold. Firstly, a semi-quantitative description of the formation of secondary phases formed between LCM and CSZ is presented. Phase distributions as well as the chemical composition of the different phases are

TABLE I Atomic ratio of cations in as synthesized $La_{1-x}Ca_xMnO_3$ powders and ratio between A- and B-site cations in LCM after reaction with CSZ at 1350 °C for 120 h

Nominal x in $La_{1-x}Ca_xMnO_3$	Measured La:Ca:Mn	$\frac{Ca+La}{Mn+Zr}$ after 120 h at 1350 °C
0.0	1.03:0.00:1	1.02
0.2	0.78:0.20:1	1.02
0.3	0.73:0.30:1	1.03
0.4	0.57:0.39:1	1.04
0.6	0.42:0.57:1	1.04

reported. Secondly, the development of the microstructure of the powder mixtures will be discussed and related to the reaction mechanism.

2. Experimental procedures

Sub-micron, stoichiometric LCM-powders containing 0, 20, 30, 40, and 60 mole% Ca on La-site were prepared by means of the glycine/nitrate method [11]. In addition, nonstoichiometric powder with composition $La_{0.75}Ca_{0.2}MnO_3$ was prepared. A molar ratio of 0.65 between glycine and nitrate was found appropriate for producing single-phase perovskite compounds except for the sample containing 60 mole % of Ca on La-site where a molar ratio of 0.55 was used. The glycine and nitrates ($La(NO_3)_3 \cdot 6H_2O$, $Mn(NO_3)_2 \cdot 4H_2O$, $Ca(NO_3)_2 \cdot 4H_2O$, $ZrO(NO_3)_2 \cdot 2H_2O$) were supplied by Merck AG and had a purity of 98.5%. The composition of the powders was measured by Atom Scan 16 ICP-AES Spectrometry (Thermo Jarrell Ash Corp., USA) (Table I). The $La_{1-x}Ca_xMnO_3$ samples with $x = 0$ and 0.3 have a slight B-site (Mn) deficiency, while the rest of the samples have a slight B-site excess relative to the ideal perovskite stoichiometry. The raw powders were calcined in air for 24 h at 1000 °C. The BET specific surface area of the calcined powders was in the range 2.1–5.5 m^2/g, which is consistent with an average particle diameter of 0.2–0.4 μm assuming that the particles are spherical. CSZ-powder with 17 mole % CaO was supplied from Seattle Specialty Ceramics, USA, and had a purity of 99.9%. The BET specific surface area was $>3\,m^2/g$ and the average grain-size was $<1\,\mu$m. The LCM/CSZ samples were prepared in the form of powder mixtures giving a large contact area between the two phases. A 1:1 mass ratio of the LCM and CSZ-powders was mixed by dry ball-milling for 8 h using yttria stabilized zirconia as ball material. The powder mixtures were uniaxially pressed at 90 MPa and fired in air or in reducing atmosphere ($p_{O_2} \sim 10^{-6}$ atm) at temperatures between 1000 and 1350 °C for periods between 1 min and 120 h. The average heating and cooling rate of the samples fired for 120 h was 200 °C/h. Thus, the samples spent 3 h above 1000 °C during heating and cooling from 1350 °C. The samples fired for 1 h were subjected to a heating rate of approximately 4200 °C/h and a cooling rate of approximately 2700 °C/h, giving an excess time above 1000 °C of 13 min. The samples fired for 15 min or less, were placed directly into the furnace at 1350 °C and removed at the same temperature giving nearly no excess time above 1000 °C. Shrinkage/expansion of pellets prepared by cold isostatic pressing (CIP) at 200 MPa were measured by dilatometry (Netzsch 402E).

Samples with compositions $La_{0.14}Ca_{0.05}Mn_{0.14}Zr_{0.26}O$ and $La_{0.11}Ca_{0.10}Mn_{0.15}Zr_{0.24}O$, corresponding to a 1:1 mass ratio of $La_{1-x}Ca_xMnO_3$ ($x = 0$ and $x = 0.3$) and $Ca_{0.17}Zr_{0.83}O_{1.83}$, were prepared by means of the glycine/nitrate method with a glycine/nitrate ratio of 0.65. Equilibrium phase composition was expected to be reached fast in these samples relative to the phase composition of the LCM/CSZ powder mixtures described previously. These samples are labeled "atomic mix" in the following. The samples were fired in air for 120 h at 1350 °C with a heating and cooling rate of 200 °C/h.

The heat treated powder samples were subjected to powder X-ray diffraction (XRD), Philips PW 1050/25, and Siemens D5005, using $Cu_{K\alpha}$ radiation and a scan rate of respectively $0.005°/s$ and $0.05°/s$. Prior to XRD, the samples were crushed and mixed with 20 wt % Si-powder, being an internal standard for d-value calibration. The semi-quantitative amounts of secondary phases present in the samples are expressed by the ratio between the 100% intensity reflection for the secondary phases LZ (222 reflection, $M_{hkl} = 8$), CZ (121 reflection, $M_{hkl} = 8$), and MnO (200 reflection, $M_{hkl} = 6$) and the 100% reflection of the CSZ-phase (111 reflection, $M_{hkl} = 8$), taking plane multiplicity factors, M_{hkl} [12], into account.

The development of the microstructure of the samples was studied by scanning electron microscopy (SEM, Zeiss DSM 940) and transmission electron microscopy (TEM, Philips CM30, 300 kV) both equipped with energy dispersive spectroscopy (EDS) systems for microanalysis. Samples for TEM analysis were prepared by sectioning, polishing, and Ar-ion beam thinning.

3. Results and discussion

3.1. Formation of secondary phases

Formation of secondary phases at the interface between LCM and CSZ in air at 1350 °C may be represented by the simplified reactions:

$$12ZrO_2(s) + 12LaMnO_3(s) = 6La_2Zr_2O_7(s) + 4Mn_3O_4(s) + O_2(g) \quad (1)$$

$$3ZrO_2(s) + 3CaMnO_3(s) = 3CaZrO_3(s) + Mn_3O_4(s) + O_2(g) \quad (2)$$

where calcia in the zirconia has been neglected for simplicity. XRD analysis revealed that the structure of LM in the $LaMnO_3$/CSZ powder mixture had changed from rhombohedral to orthorhombic already after 10 min at 1350 °C, indicating a reductive reaction as (1). For $LaMnO_{3+\delta}$ (La:Mn = 1:1) the room temperature structure has been found to change from rhombohedral to orthorhombic below about 25% Mn^{4+} [13]. However, the dissolution of Zr on B-site in $LaMnO_{3+\delta}$ may also contribute to the destabilization of rhombohedral $LaMnO_{3+\delta}$. The manganese oxide stable in

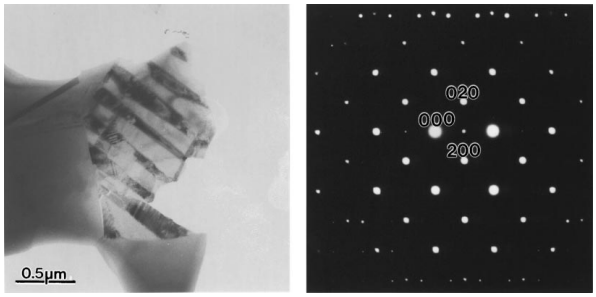

(a) (b)

Figure 1 Bright field image of a Mn_3O_4 grain showing (a) extensive twinning, and (b) [0 1 0] zone-axis pattern.

air at 1350 °C is Mn_3O_4 according to Fritsch *et al*. [14]. Grains of pure Mn_3O_4 were observed by TEM in the $La_{0.4}Ca_{0.6}MnO_3$/CSZ powder mixture fired for 1 h at 1350 °C. The Mn-oxide grains were extensively twinned and, therefore, easily recognized (Fig. 1a). The Mn_3O_4 grains were characterized by selected area electron diffraction (SAED) (Fig. 1b) and by EDS, giving an O to Mn ratio of 1.329, which is almost identical to the O to Mn ratio of 1.333 in Mn_3O_4. Formation of manganese oxide was not observed in any other heat treated powder mixture of LCM and CSZ in air. The absence of manganese oxide is explained by the diffusion of Mn into CSZ and the dissolved Mn in the secondary phases LZ and CZ, as will be shown in the following sections. Formation of secondary phases at the interface between LCM and CSZ is, therefore, mainly governed by the thermodynamic properties of the zirconate phases.

The semi-quantitative amounts of secondary phases formed at 1350 °C after 120 h for all the LCM-compositions are summarized in Fig. 2a. Only minor amounts of secondary phases were observed in the $La_{1-x}Ca_xMnO_3$/CSZ, $x = 0.2$ and 0.4, samples. For $x = 0.3$, there was no indication of secondary phases. Compared to the LSM/YSZ system studied by Wiik *et al*. [9], the semi-quantitative amounts of secondary phases in the present LCM/CSZ system are about 50% lower. The LCM/CSZ system is, therefore, more stable against formation of secondary phases than the LSM/YSZ system as expected from the reduced thermodynamic driving force by replacing yttria in zirconia with calcia.

Due to the relatively large amounts of secondary phases formed in the samples with $x = 0$ and $x = 0.6$, these two samples were more carefully studied. The relative amounts of LZ and CZ in these two samples are presented in Fig. 2b as a function of heat treatment time and temperature. The amounts of CZ in $La_{0.4}Ca_{0.6}MnO_3$/CSZ and LZ in $LaMnO_3$/CSZ are almost constant after 1 h at 1350 °C, indicating that all powder mixtures are in equilibrium after 1 h at 1350 °C. Taimatsu *et al*. [6] and Kaneko *et al*. [7], however, observed that an induction period was necessary for the formation of LZ in LM(stoichiometric)/YSZ diffusion couples. LZ-phases were rarely observed at reaction interfaces at temperatures below 1400 °C for 100 h. However, in our model system the reaction is much faster due to the small particle size of the two primary phases and the large contact area between the two phases. However,

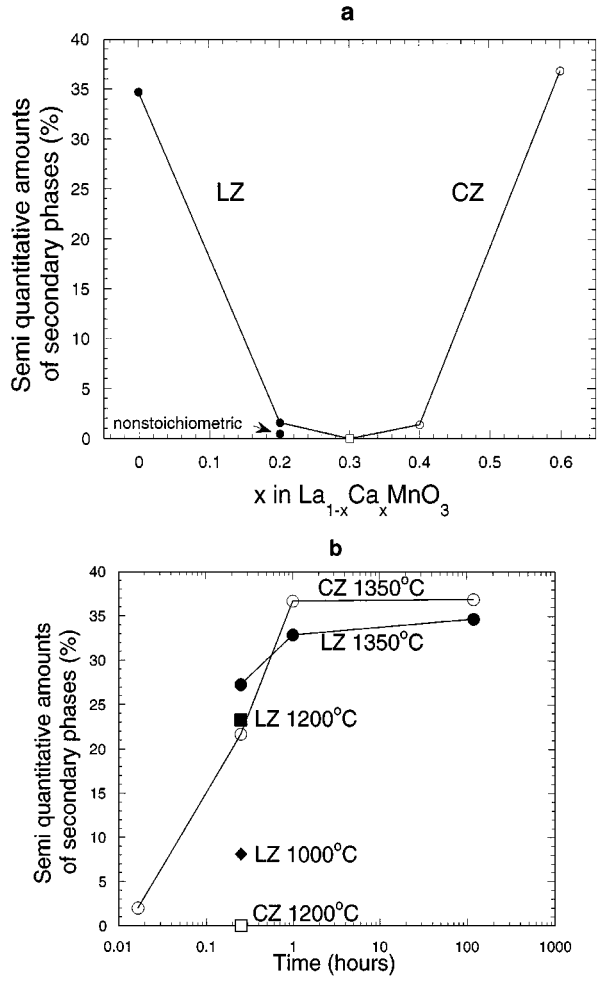

Figure 2 (a) Semi-quantitative analysis of the amounts of secondary phases (LZ and CZ) formed in powder mixtures of LCM and CSZ as a function of mole % Ca in LCM after 120 h at 1350 °C, and (b) as a function of temperature and time for the $La_{0.4}Ca_{0.6}MnO_3$/CSZ and $LaMnO_3$/CSZ samples. The open square describes no indication of secondary phases. The nonstoichiometric sample corresponds to $La_{0.75}Ca_{0.2}MnO_3$/CSZ. The uncertainty in each point is ∼±1%.

for powder mixtures in the LSM/YSZ system, Wiik *et al*. [9] observed that the time necessary to achieve equilibrium phase composition at 1350 °C was clearly dependent on the Sr-content of LSM. For the samples with $x = 0.3$, 0.4, and 0.6, equilibrium was established after 1–3 h at 1350 °C, while for the $LaMnO_3$/YSZ powder, mixture equilibrium was established after 70 h at 1350 °C. Thus, equilibrium is established faster in the LCM/CSZ system than in the LSM/YSZ system. This might be due to the lower number of chemical components in the present system.

All powder mixtures were found to be more reactive in reducing atmosphere ($p_{O_2} \sim 10^{-6}$ atm) than in air. Both CZ and LZ were found in all powder mixtures ($x = 0$, 0.3, 0.6) after 120 h at 1350 °C in reducing atmosphere. The amount of LZ decreases, and the amount of CZ increases with increasing amount of Ca in LCM, as expected (Fig. 3). However, note that there are significant amounts of LZ in $La_{0.4}Ca_{0.6}MnO_3$/CSZ and CZ in $LaMnO_3$/CSZ. EDS-results obtained for the CZ, LZ, and CSZ phases are shown in Table II. Yokokawa *et al*. [8] proposed that a high oxygen potential was needed for the formation of LZ at the YSZ/LM interface. CSZ is observed to persist in all three powder

TABLE II Chemical composition of CZ, CSZ, and LZ in powder mixture samples fired for 120 h at 1350 °C in reducing atmosphere ($p_{O_2} \sim 10^{-6}$ atm)

Phase		CZ		
$La_{1-x}Ca_xMnO_3$	La	Mn	Zr	Ca
x = 0.0	11.8 ± 1.0	11.6 ± 0.7	47.4 ± 0.7	29.3 ± 1.2
x = 0.3	12.4 ± 1.6	12.5 ± 1.2	46.6 ± 1.4	28.5 ± 1.2
x = 0.6	12.0 ± 1.3	12.5 ± 0.6	46.4 ± 0.9	29.2 ± 0.9
Phase		CSZ		
$La_{1-x}Ca_xMnO_3$	La	Mn	Zr	Ca
x = 0.0	6.0 ± 0.5	7.5 ± 1.3	75.9 ± 1.0	10.8 ± 0.6
x = 0.3	6.1 ± 0.7	8.7 ± 0.7	74.2 ± 1.1	11.0 ± 0.4
x = 0.6	5.5 ± 0.4	8.6 ± 1.8	74.1 ± 1.6	11.8 ± 0.7
Phase		LZ		
$La_{1-x}Ca_xMnO_3$	La	Mn	Zr	Ca
x = 0.0	36.1 ± 1.3	1.0 ± 0.9	59.0 ± 1.6	3.3 ± 1.4
x = 0.3	35.8 ± 0.9	1.9 ± 1.3	58.6 ± 0.4	3.7 ± 0.3
x = 0.6	36.1 ± 0.7	2.1 ± 0.7	58.4 ± 0.3	3.4 ± 0.4

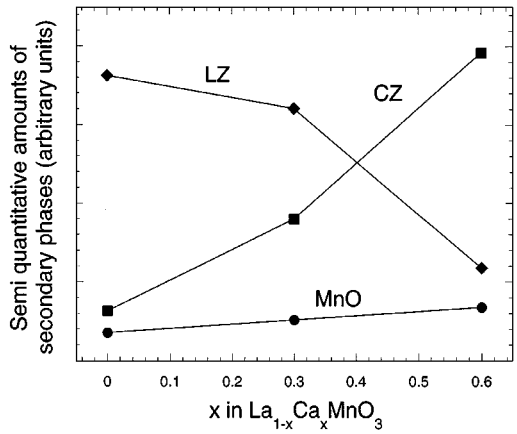

Figure 3 Semi-quantitative analysis of the amounts of secondary phases (LZ, CZ, and MnO) formed in powder mixtures of LCM and CSZ as a function of mole % Ca in LCM after 120 h at 1350 °C in reducing atmosphere ($p_{O_2} \sim 0^{-6}$ atm).

mixtures during firing for 120 h at 1350 °C. The LM/LCM phase, however, is partly found to be dissolved in the other phases and partly to be transformed to MnO, which is the stable manganese oxide at $P_{O_2} \sim 10^{-6}$ atm and 1350 °C [14]. At 1350 °C, LM decomposes at $p_{O_2} < 2.4 \cdot 10^{-10}$ atm according to thermodynamical data given by Nakamura *et al*. [15]. Hence, the reducing atmosphere used here ($p_{O_2} \sim 10^{-6}$ atm) is almost four decades higher than the decomposition pressure. After 1 h at 1350 °C, LM/LCM is observed in all three samples, however, after 120 h at 1350 °C some perovskite is left only in the $La_{0.7}Ca_{0.3}MnO_3$/CSZ powder mixture, indicating that this composition is the most stable also in reducing atmosphere. According to Gibbs phase rule, $p + f = c + 2$, where p is the number of phases, f is the number of degrees of freedom, c is the number of components (Ca, La, Mn, O, Zr ⇒ c = 5), at $p_{O_2} = 10^{-6}$ atm, and T = 1350 °C the maximum number of phases in equilibrium is 5 (4 solid phases + O_2(g)). Thus, due to the presence of five solid phases (LCM, CSZ, CZ, LZ, MnO) in $La_{0.7}Ca_{0.3}MnO_3$/CSZ, this powder mixture is not in equilibrium after 120 h at 1350 °C in reducing atmosphere.

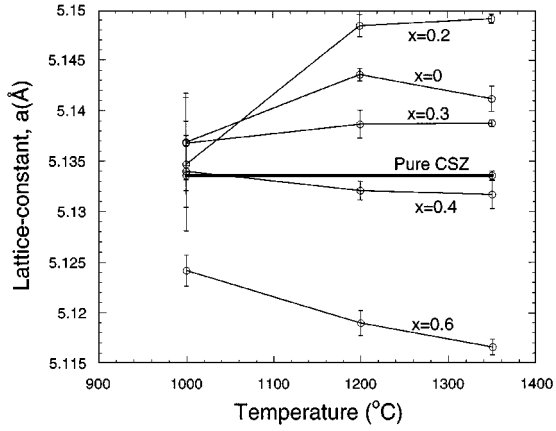

Figure 4 CSZ lattice parameter versus temperature for $La_{1-x}Ca_xMnO_3$/CSZ (x = 0, 0.2, 0.3, 0.4, and 0.6) powder mixtures fired for 15 min. The lattice parameter for pure CSZ (a = 5.133(6) Å) was also measured by XRD.

3.2. Characterization of phases

The lattice parameter for cubic CSZ was observed to depend on the composition of LCM, and is given as a function of temperature for all powder mixtures fired in air for 15 min in Fig. 4. Already after 15 min at 1000 °C the CSZ lattice parameter for some of the mixtures deviates considerably from pure CSZ, which demonstrates that considerable inter-diffusion between the primary phases has already occurred. The correlation between chemical composition and lattice parameter of CSZ and LCM in powder mixtures fired at 1350 °C for 120 h is illustrated in Fig. 5. It is known that all the cations in the present system possess considerable solid solubility in the cubic form of ZrO_2 [16–18]. The solubility of MnO in ZrO_2 is ∼20 wt % at reducing conditions [18]. It is also known that Mn ($r_{Mn^{2+}} = 0.89$ Å [19]) causes a contraction of the CSZ unit cell, while Ca ($r_{Ca^{2+}} = 1.12$ Å [19]) and La ($r_{La^{3+}} = 1.18$ Å [19]) cause an expansion of the unit cell when all elements retain a cubic coordination (CN = 8). The CSZ-lattice is seen to expand to a maximum at x = 0.20 in $La_{1-x}Ca_xMnO_3$ when the amount of Ca increases and the Mn and La contents are nearly constant (Fig. 5a). The lattice is then seen to contract due to decreasing La-content suppressing the expanding effect of Ca. 60 mole % Ca on La-site gives the most contracted lattice with high Mn and low La-content. The significant concentrations of Mn and La (2–8 at %) in CSZ (Fig. 5a) and Zr (2–5 at %) in LCM (Fig. 5b) indicate that in addition to surface diffusion, volume diffusion is a significant mechanism for mass transport.

The A/B-ratio of LCM has been estimated for all LCM/CSZ powder mixtures fired at 1350 °C for 120 h assuming Zr to occupy Mn-site. The results indicate that the initial 1:1 ratio between A and B-site cations is preserved during the reaction (Table I and Fig. 5b) as opposed to the LSM/YSZ system where A-site deficiency of $LaMnO_3$ and $La_{0.7}Ca_{0.3}MnO_3$ was observed when exposed to cubic zirconia [9]. The A/B ratio is preserved due to the simultaneously increasing contents of Ca and Zr on, respectively, A- and B-site in the perovskites having a low nominal Ca-content (Fig. 5b). Thus, due to the stoichiometry, the perovskite in the

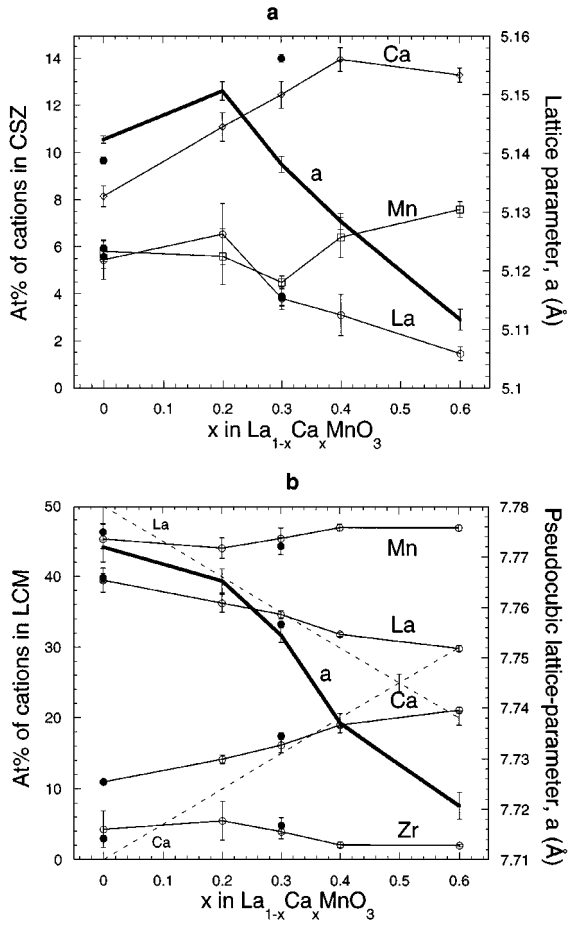

Figure 5 Chemical composition (left ordinate) and lattice parameter (right ordinate) of the CSZ-phase (a) and the LCM-phase (b) in terms of mole % of Ca in LCM for samples fired at 1350 °C for 120 h. The lattice parameter of pure CSZ (17 mole % CaO) is 5.133 (6) Å. Open symbols describe powder mixtures and filled circles describe "atomic mix" samples. The dotted lines indicate the nominal amounts of Ca and La in pure LCM. Note that the initial content of Ca in CSZ is 17 mole %.

LCM/CSZ system has a lower Gibbs energy than the perovskite in the LSM/YSZ system, which is consistent with an increased stability of the LCM/CSZ interface.

For the intermediate mixture $La_{0.7}Ca_{0.3}MnO_3$/CSZ, the initial 0.7:0.3 ratio between La and Ca in LCM is almost preserved (0.65:0.3) indicating negligible net diffusion of La and Ca (Fig. 5b), confirming the stability of this interface. There is, however, some inter-diffusion of Mn and Zr giving rise to an expansion of the pseudo-cubic lattice parameter of LCM in $La_{0.7}Ca_{0.3}MnO_3$/CSZ compared to the pseudo-cubic lattice parameter, a = 7.732 Å [20], of pure $La_{0.7}Ca_{0.3}MnO_3$. It is therefore proposed that the major reason for the expansion of the cell volume of all LCM-phases exposed to CSZ is due to the presence of Zr on Mn-sites ($r_{Mn^{3+}} = 0.65$ Å for CN = 6 and $r_{Zr^{4+}} = 0.72$ Å for CN = 6 [19]). Concerning the stability of the $La_{0.7}Ca_{0.3}MnO_3$/CSZ interface, it should be noted from Fig. 5a that the Mn concentration has a minimum for x = 0.3, indicating the lowest activity of Mn-oxide and the most stable LCM/CSZ interface for this composition of LCM. Compared to the nominal content of Ca in pure LCM (Fig. 5b), Ca is seen to diffuse into LCM for x < 0.3 and out off LCM for x > 0.3 due to the reaction with CSZ, indicating that the chemical potential for Ca is identical in LCM and CSZ for x ≈ 0.3. The fact that Ca diffuses into the CSZ-phase for x > 0.3 explains why CZ is formed in these samples, while in the samples with x < 0.3, the CSZ-phase becomes Ca-deficient relative to the initial composition, giving no CZ. However, to compensate for the A-site excess caused by the diffusion of Ca into LCM for x < 0.3, LZ is formed reducing the concentration of La in LCM below the value in pure LCM (Fig. 5b). In this way the initial 1:1 ratio between A- and B-site cations is preserved during the reaction.

The unit cell parameters for the secondary phases LZ and CZ were observed to deviate considerably from literature data [21, 22]. The estimated cubic lattice parameter of LZ after firing LM/CSZ for 1 and 120 h at 1350 °C is shown in Fig. 6a. The lattice parameter is considerably lower than reported for pure LZ (a = 10.793 Å [21]). The Zr/La ratio equals 1.7 both after 1 and 120 h (Fig. 6a). This result is in accordance with the spread in the Zr/La ratio from 1.3 to nearly 2, which was observed in the pyrochlore grains formed at LSM/YSZ boundaries by Clausen *et al*. [23]. The Zr/La ratio is 1 in the ideal pyrochlore structure. Based on the ionic radius of La^{3+} ($r_{La^{3+}} = 1.18$ Å CN = 8 [19]) and Zr^{4+} ($r_{Zr^{4+}} = 0.72$ Å CN = 6 [19]) in the pyrochlore structure, the unit cell is expected to contract when the

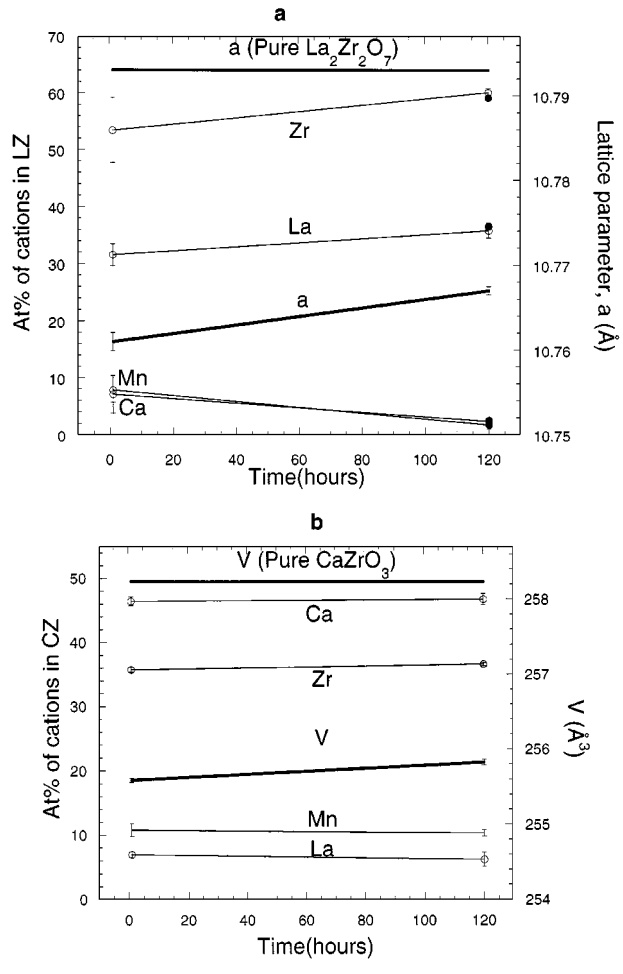

Figure 6 Chemical composition (left ordinate) and lattice parameter/unit cell volume (right ordinate) of the secondary phases LZ (a) and CZ (b) fired at 1350 °C for 120 h. Open circles describe powder mixtures, and filled circles describe "atomic mix" samples.

Zr/La ratio is raised as observed here. It is seen that the lattice parameter is virtually time independent, consistent with a nearly time independent composition. EDS analysis demonstrates the presence of 2–8 at % Ca and Mn in LZ. Concerning the mass balance of Ca in the LM/CSZ powder mixture, half of the amount of Ca-ions diffusing out of CSZ is found to enter LM, while the other half is dissolved in LZ.

The orthorhombic unit cell volume of CZ versus heat treatment time of $La_{0.7}Ca_{0.3}MnO_3$/CSZ fired at 1350 °C is shown in Fig. 6b. A considerable deviation from the unit cell volume of pure CZ ($V = 258.23$ Å^3 [22]) is evident. The contracted lattice is probably due to the considerable content of La and Mn on A- and B-sites, respectively. At 1350 °C the composition is seen to be almost time independent after 1 h. The small variation in unit cell volume with respect to time, shown in Fig. 6b, confirms the nearly time independent behavior of the composition. The EDS analysis suggests that CZ has a complex stoichiometry. Significant amounts of all the possible cations are found in the CZ phase. The perovskite structure of CZ can tolerate only a few per cent of vacancies at the A- or B-site. In the $La_{0.7}Ca_{0.3}MnO_3$/CSZ mixture, the A/B ratio of CZ is 0.998 and 0.996 in the samples fired for 1 and 120 h, respectively, assuming the La^{3+} ions to occupy A-sites and Mn^{4+} ions to occupy B-sites in the perovskite structure.

The chemical compositions of the different phases formed in the "atomic mix" samples after 120 h at 1350 °C are shown as filled circles in Figs 5 and 6a. The atom % of the different elements in each phase of the powder mixtures and "atomic mix" samples are consistent within the standard deviation. The chemical composition of the phases and analysis of the formation of secondary phases as a function of temperature and time (Fig. 2b) reveal that all the powder mixtures are in equilibrium after 1 h at 1350 °C in air.

3.3. Microstructure and reaction mechanism

To obtain information about nucleation and growth of the LZ and CZ phases, the LM/CSZ and $La_{0.4}Ca_{0.6}MnO_3$/CSZ samples were studied by TEM after a short firing period; respectively 10 min and 1 min at 1350 °C (Fig. 7). The formation of secondary phases in lanthanum manganite (LXM, X = Ca, Sr)/YSZ systems has been studied by several researchers [1–7]. The nucleation is found to occur at the LXM/YSZ interface, but there is a disagreement on whether the grains of the secondary phases grow into the YSZ-phase, the LXM-phase or both. In our LCM/CSZ system, we observed nucleation of LZ/CZ at the LCM/CSZ interface and triple-points as well as further growth mainly into the CSZ-phase. Rounded grains of LZ and CZ, respectively, are seen in L(C)M/CSZ triple-points in Fig. 7a and b. A reaction mechanism has been proposed by Taimatsu *et al*. [6] for the formation of LZ at the YSZ/$La_{1-x}Ca_xMnO_3$ (x = 0, 0.1, 0.2) boundary. Mn ions are assumed to diffuse faster than La-ions into YSZ and subsequently the residual La_2O_3 reacts with ZrO_2 to form LZ. La and Mn ions diffuse unidirectionally

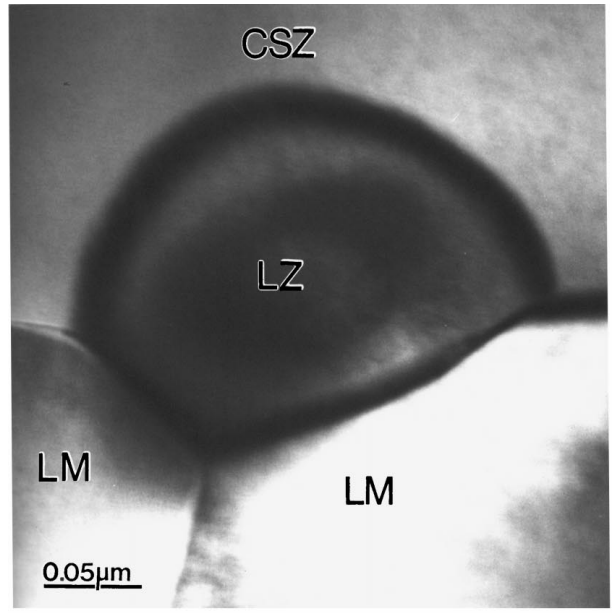

(a)

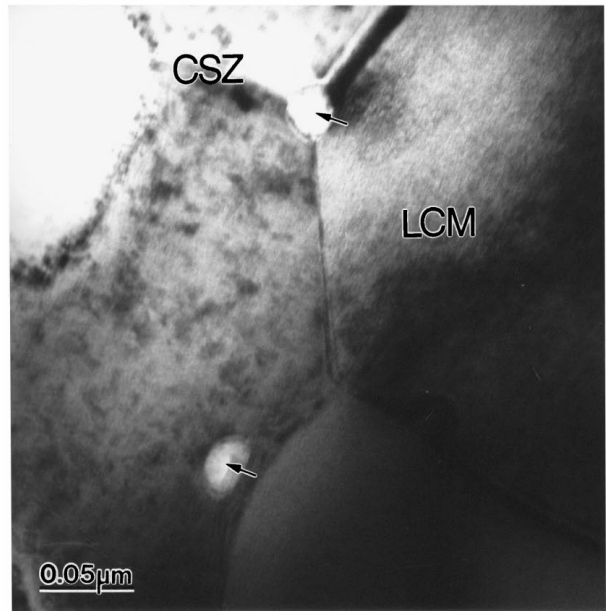

(b)

Figure 7 (a) TEM images of $LaMnO_3$/CSZ fired for 10 min at 1350 °C and (b) $La_{0.4}Ca_{0.6}MnO_3$/CSZ fired for 1 min at 1350 °C.

through the LZ layer, which grows at the LZ/YSZ interface. Mitterdorfer *et al*. [24] found that the growth of LZ in a LSM/YSZ diffusion couple was initially limited by surface diffusion of La^{3+} and Zr^{4+}, which is much faster than bulk diffusion of these elements through LZ. Accordingly, it is assumed that LZ and CZ grow by surface diffusion of Ca^{2+} and La^{3+} in addition to Zr^{4+}. The observation that LZ grows mainly into the CSZ-phase is in accordance with the reaction mechanism proposed by Taimatsu *et al*. [6]. However, no La_2O_3 is formed in the powder mixtures due to the fact that the CSZ-phase is saturated by Mn before the solubility limit for La_2O_3 is reached. However, the activity of La_2O_3 in stoichiometric LCM becomes sufficiently high during reaction with CSZ to cause nucleation of LZ. Accordingly, A(La)-site deficient perovskites, like $La_{0.75}Ca_{0.20}MnO_3$, cause a lower activity of La_2O_3 and thus a more stable interface with CSZ. In the A-site deficient

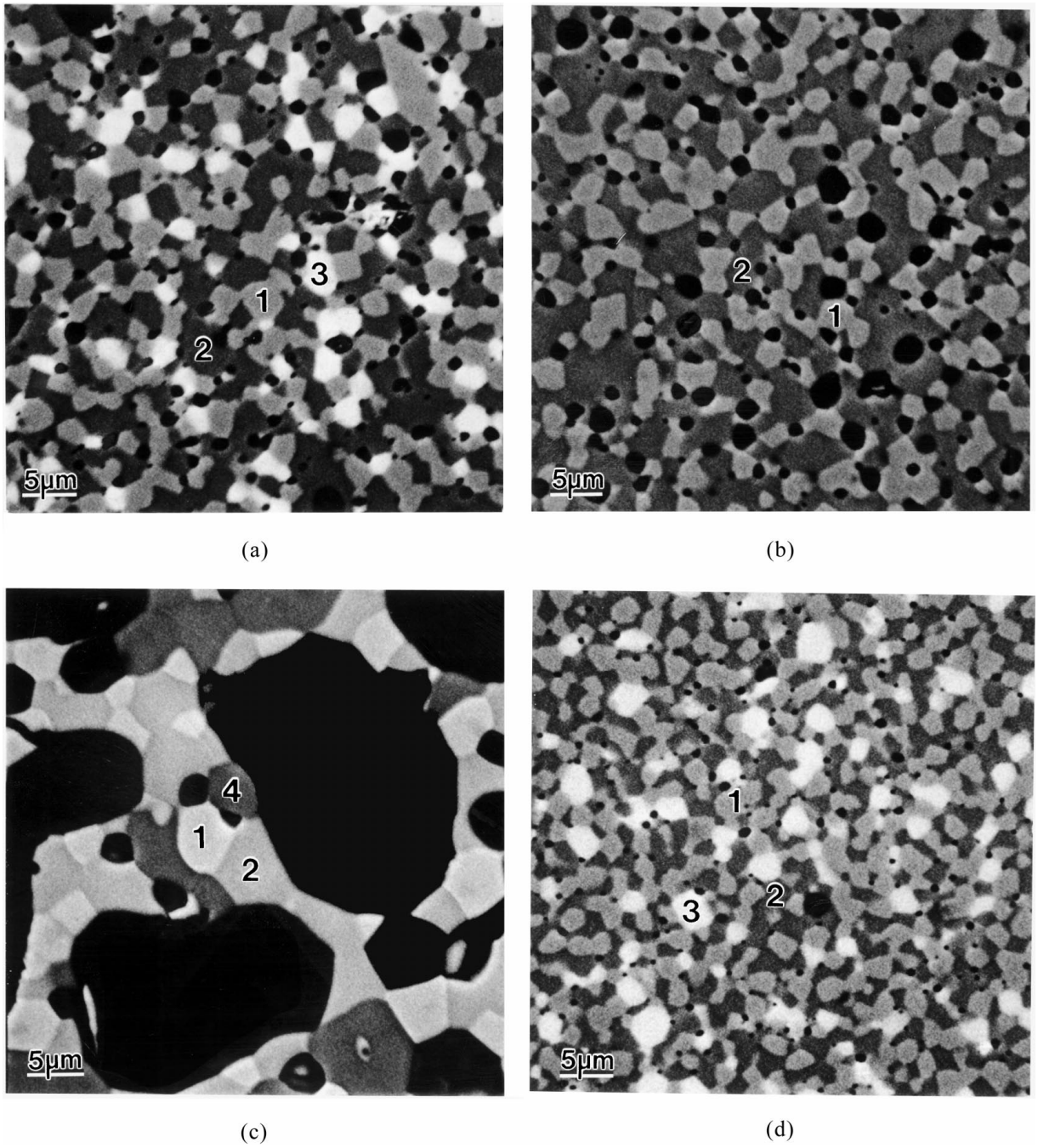

Figure 8 (a) SEM backscatter images of $LaMnO_3$/CSZ, (b) $La_{0.7}Ca_{0.3}MnO_3$/CSZ, and (c) $La_{0.4}Ca_{0.6}MnO_3$/CSZ powder mixtures fired for 120 h at 1350 °C. (d) SEM backscatter image of $LaMnO_3$/CSZ "atomic mix" sample fired for 120 h at 1350 °C. (e) SEM backscatter images of $LaMnO_3$/CSZ, (f) $La_{0.7}Ca_{0.3}MnO_3$/CSZ, and (g) $La_{0.4}Ca_{0.6}MnO_3$/CSZ powder mixtures fired for 120 h at 1350 °C in reducing atmosphere ($p_{O_2} \sim 10^{-6}$ atm). 1 = LCM, 2 = CSZ, 3 = LZ, 4 = CZ. *(Continued).*

$La_{0.75}Ca_{0.2}MnO_3$/CSZ powder mixture there were only traces of LZ. The amount was significantly smaller than in the stoichiometric $La_{0.8}Ca_{0.2}MnO_3$/CSZ sample (Fig. 2a), consistent with the observation by Clausen *et al.* [23].

The further development in microstructure was studied by SEM. Before chemical equilibrium is established (i.e., during the first hour at 1350 °C), the development of the microstructure in all samples is characterized by formation of secondary phases (except for $x = 0.3$), pore-coarsening and moderate grain-growth. After 15 min at 1350 °C, the grains are still sub-micron, and even after 1 h at 1350 °C all samples, except for $x = 0.6$, have grain sizes of ∼1–2 μm. After chemical equilibrium is established, the development of the microstructure in all samples is characterized by extensive grain-growth and pore-coarsening. The microstructures of the $La_{1-x}Ca_xMnO_3$/CSZ, $x = 0$, 0.3, and 0.6, samples fired at 1350 °C for 120 h are given in Fig. 8a–c. The LM/CSZ sample demonstrates a sintered structure with low porosity after 120 h. Grain growth has occurred to a great extent, giving about a tenfold increase in grain size for both LM and CSZ. In addition, LZ grains with about the same size as the LM and CSZ grains are observed. In the $La_{0.7}Ca_{0.3}MnO_3$/CSZ sample, no secondary phases were detected by SEM or TEM, confirming the results from the XRD analysis. The sample containing LCM with 60 mole % Ca on

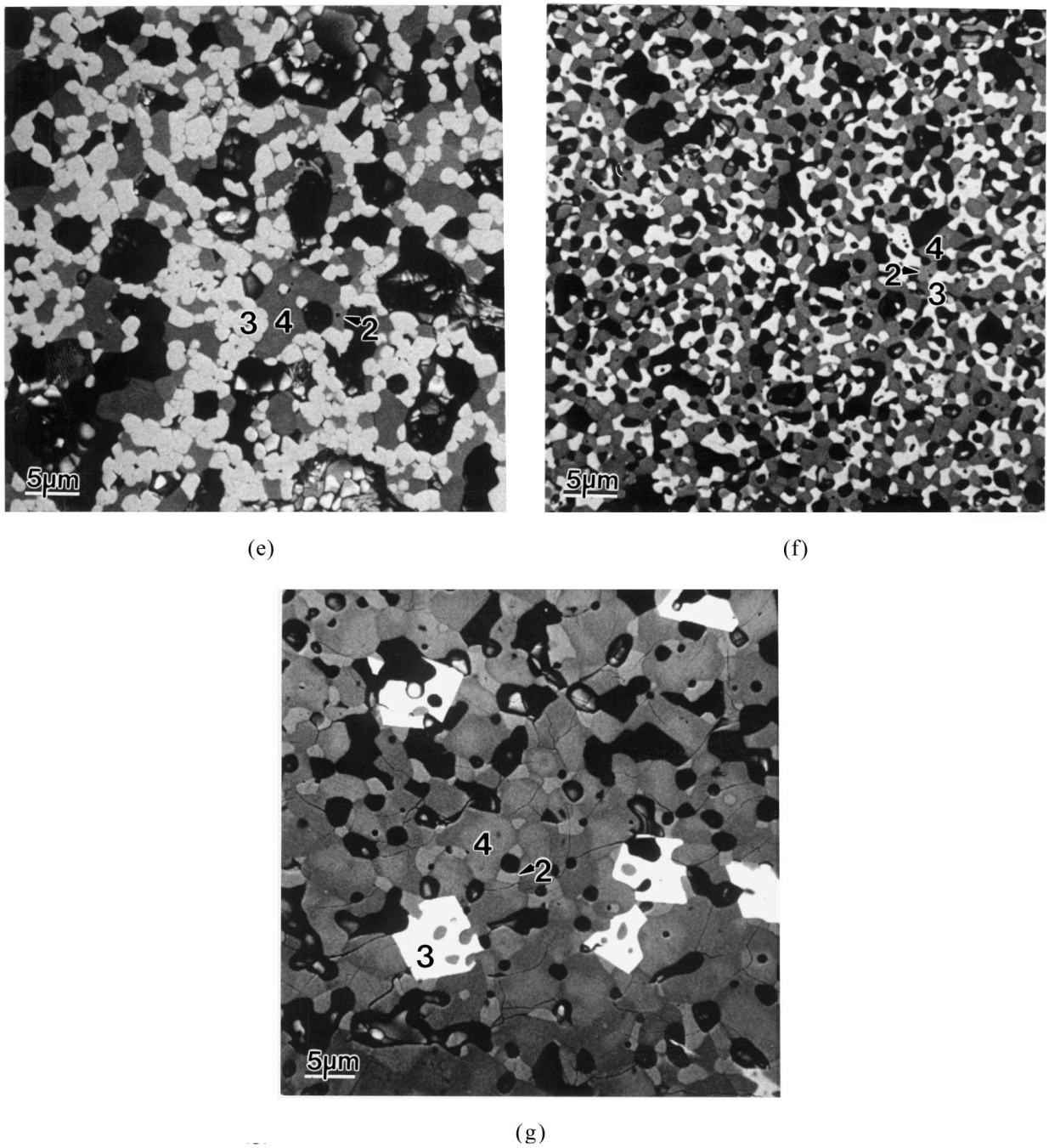

(e) (f) (g)

Figure 8 (Continued).

La site displays a highly porous structure after 120 h (Fig. 8c) with a pore size up to about 40 μm and a grain size up to about 5 μm. The distance between the pores is only a few grain-diameters. The perovskite phase, CZ, and CSZ demonstrate a modest grain growth compared to the pore-coarsening.

The effect of the pore-coarsening on the density of the powder mixture $La_{0.4}Ca_{0.6}MnO_3$/CSZ is shown in Fig. 9. Pore-coarsening can in general take place by an Ostwald ripening process, if the entrapped gas in the pores is soluble in the material, or by coalescence. However, the reduction in density due to these mechanisms is normally in the order of a few percent [25], giving much less reduction in density than observed in Fig. 9. Thus, evolution of oxygen from LCM during heating [26] and during formation of LZ and CZ caused by the reduction of Mn^{4+}/Mn^{3+} to Mn^{3+}/Mn^{2+} ((1) and (2)), must contribute to the pore-coarsening in these samples. The increase in pore-diameter follows a $t^{\frac{1}{2.9}}$ law (Fig. 9), indicating that pore-coarsening takes place mainly via an Ostwald ripening process [25]. The fact that the CZ-phase has a larger molar volume than the two primary phases also contributes to the volume expansion, but this effect is small compared to the effect of pore-coarsening. Given that the LCM/CSZ grain boundary is permeable (i.e., exhibiting both anionic and electronic conductivity), oxygen will be transported from the smaller pores to the larger pores via the grain-boundaries in accordance with the pore-coarsening mechanism proposed for LSM/YSZ powder mixtures by Wiik *et al*. [9]. Assuming all $LaMnO_{3.15}$ to be reduced to $LaMnO_3$, the oxygen evolved from the perovskite during heating is larger by a factor of 100 than needed to explain the expansion of the powder

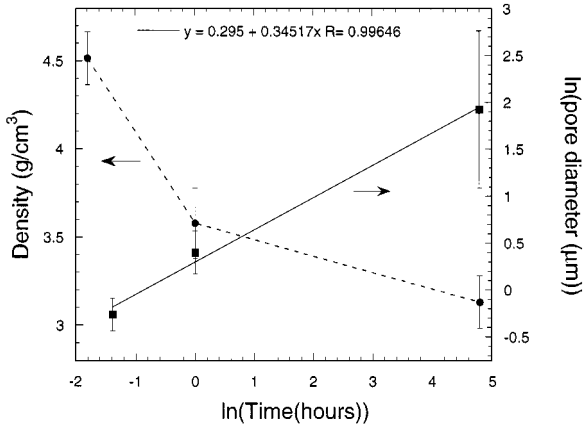

Figure 9 Density (left ordinate) and pore diameter (right ordinate) versus sintering time at 1350 °C for $La_{0.4}Ca_{0.6}MnO_3$/CSZ. The pore-diameter reported for each sample is the average of 50 pores. The green density of the $La_{0.4}Ca_{0.6}MnO_3$/CSZ sample was 2.65 g/cm^3. The dotted line through the relative density points is a guide to the eye.

mixtures. Similarly, the evolution of oxygen during formation of LZ and CZ, assuming all the perovskite phase transformed to MnO, is larger than the number of moles needed for the expansion by a factor of 1000. Thus, most of the oxygen is transported out of the material during the heating period when there is open porosity. However, when the pores close, the evolution of oxygen will cause an expansion of the material. Dilatometry showed the linear expansion to start immediately after the temperature reached 1350 °C, indicating the closure of the pores. The evolution of oxygen from the perovskite is supposed to equilibrate shortly after the temperature reaches 1350 °C. However, the evolution of oxygen due to reactions (1) and (2) will continue for about 1 h after the temperature has reached 1350 °C because of the formation of secondary phases (Fig. 2b). Further expansion after 1 h must therefore be caused by pore ripening. An illustration of the pore ripening process is shown in Fig. 10. The observation of increasing pore-coarsening with increasing amount of Ca in LCM indicates increasing oxygen evolution with increasing amount of Ca. This observation supports reactions (1) and (2).

The microstructure of the "atomic mix" sample LM/CSZ fired at 1350 °C for 120 h is given in Fig. 8d. Comparing this micrograph with that in Fig. 8a, it is

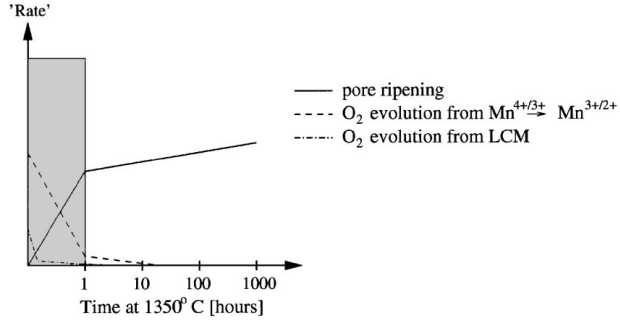

Figure 10 Relative "rates" of pore ripening and O_2 producing processes during firing at 1350 °C. During the first hour, oxygen evolution contributes to the pore-coarsening, later only pore-ripening.

evident that the phase-distribution and the grain size are very much alike in the powder mixture and the "atomic mix" sample. Also, the porosity is about the same, except for a slightly larger average pore diameter in the powder mixture. Similar results were found for the other "atomic mix" samples.

Micrographs of the $La_{1-x}Ca_xMnO_3$/CSZ, x = 0, 0.3, and 0.6, samples fired at 1350 °C for 120 h in reducing atmosphere ($p_{O_2} \sim 10^{-6}$ atm) are given in Fig. 8e–g. It should be noted that the atmosphere strongly influences the microstructure and the phase-distribution (compare Fig. 8a–c and Fig. 8e–g). Grain growth has occurred to a greater extent in reducing atmosphere, giving about a fourfold grain size in the reduced samples compared to the samples fired in air, which is consistent with a higher reactivity in reducing atmosphere. The micrographs of the samples fired in reducing atmosphere reveal a strong correlation between the microstructure of the sintered powder mixtures and the Ca-content of the perovskite phase. The most significant difference is the shape and size of the LZ-grains, which are edged in the $La_{0.4}Ca_{0.6}MnO_3$/CSZ sample and fairly spherical in the LM/CSZ sample. LCM grains could be observed by SEM after 1 h heat treatment at 1350 °C, and the $La_{0.7}Ca_{0.3}MnO_3$/CSZ powder mixture possessed the highest amount of LCM. However, after 120 h at 1350 °C, no LCM could be detected by SEM.

Conclusively, it is probably impossible to stabilize LCM/CSZ powder interfaces in reducing atmosphere. However, in air, LCM/CSZ interfaces can be stabilized either by substituting an appropriate amount of Ca on A-site or by an appropriate amount of A-site deficiency in LCM.

4. Conclusions

Solid state reactions between sub micron powders of calcium doped lanthanum manganite and calcia stabilized zirconia have been studied by means of X-ray diffraction, electron microscopy, and energy dispersive X-ray spectroscopy. The results revealed that all the powder mixtures are in equilibrium after 1 h at 1350 °C. Thus, equilibrium is established faster in the present LCM/CSZ system than in the electrode/electrolyte system conventionally being used in SOFC (LSM and YSZ). In addition, the semi-quantitative amounts of secondary phases in the LCM/CSZ system are about 50% lower, indicating that the LCM/CSZ system is more stable against formation of secondary phases than the LSM/YSZ system. The most chemically stable interface was observed when the lanthanum manganite contained 30 mole % calcium on La-site both in air and in reducing atmosphere ($p_{O_2} \sim 10^{-6}$ atm). Reducing atmosphere was, however, observed to destabilize the interface both thermodynamically and kinetically. The microstructure of the air-sintered powder mixtures revealed an increasing degree of pore-coarsening with increasing amount of Ca in LCM. The porous microstructure supports the reductive nature of the reaction between LCM and CSZ.

Acknowledgements

The authors are grateful to the Norwegian scientific foundation VISTA for financial support and to Lisbeth Bye for preparing some of the samples. Discussions with Ragnvald Høier are acknowledged.

References

1. J. MIZUSAKI, H. TAGAWA, K. TSUNEYOSHI and A. SAWATA, *J. Electrochem. Soc*. **138** (1991) 1867.
2. J. MIZUSAKI, H. TAGAWA, K. TSUNEYOSHI, A. SAWATA, M. KATOU and K. HIRANO, *Denki Kagaku* **58** (1990) 520.
3. H. TAGAWA, J. MIZUSAKI, M. KATOU, K. HIRANO, A. SAWATA and K. TSUNEYOSHI, in Proceedings of the Second International Symposium on Solid Oxide Fuel Cells, Athens, 1991, edited by F. Gross, P. Zegers, S. C. Singhal and O. Yamamoto, p. 681.
4. Y. TAKEDA, Y. SAKAI, T. ICHIKAWA, N. IMANISHI and O. YAMAMOTO, *Solid State Ionics* **72** (1994) 257.
5. K. TSUNEYOSHI, K. MORI, A. SAWATA, J. MIZUSAKI and H. TAGAWA, *ibid*. **35** (1989) 263.
6. H. TAIMATSU, K. WADA, H. KANEKO and H. YAMAMURA, *J. Am. Ceram. Soc*. **75** (1992) 401.
7. H. KANEKO, H. TAIMATSU, K. WADA and E. IWAMOTO, in Proceedings of the Second International Symposium on Solid Oxide Fuel Cells, Athens, 1991, edited by F. Gross, P. Zegers, S. C. Singhal and O. Yamamoto, p. 673.
8. H. YOKOKAWA, N. SAKAI, T. KAWADA and M. DOKIYA, *Sci. Tech. Zirconia* **5** (1993) 752.
9. K. WIIK, C. R. SCHMIDT, S. FAALAND, S. SHAMSILI, M.-A. EINARSRUD and T. GRANDE, *J. Am. Ceram. Soc*., in print.
10. S. FAALAND, M.-A. EINARSRUD, K. WIIK, R. HØIER and T. GRANDE, in preparation.
11. L. A. CHICK, L. R. PEDERSON, G. D. MAUPIN, J. L. BATES and L. E. THOMAS, *Mater. Lett*. **10** (1990) 6.
12. R. JENKINS and R. L. SNYDER, in "X-ray Powder Diffractometry" (John Wiley & Sons, Inc., 1996) p. 77.
13. J. A. M. VAN ROOSMALEN, P. VAN VLAANDEREN, E. H. P. CORDFUNKE, W. L. IJDO and D. J. W. IJDO, *J. Solid State Chem*. **114** (1995) 516.
14. S. FRITSCH and A. NAVROTSKY, *J. Am. Ceram. Soc*. **79** (1996) 1761.
15. T. NAKAMURA, G. PETZOW and L. J. GAUCKLER, *Mat. Res. Bull*. **14** (1979) 649.
16. A. ROUANET, *Rev. Int. Hautes Temp. Refract*. **8** (1971) 161.
17. T. NOGUCHI and O. YONEMOCHI, *J. Am. Ceram. Soc*. **52** (1969) 178.
18. R. L. SHULTZ and A. MUAN, *ibid*. **54** (1971) 504.
19. R. D. SHANNON and C. T. PREWITT, *Acta Cryst.* **B25** (1968) 925.
20. S. FAALAND, K. D. KNUDSEN, M.-A. EINARSRUD, L. RØRMARK, R. HØIER and T. GRANDE, Accepted May 7 1998, *J. Solid State Chem.*, In print.
21. J. ROTH, *Res. Natl. Bur. Stand*. (U.S.) **56** (1956) 17.
22. V. P. DRAVID, C. M. SUNG, M. R. NOTIS and C. E. LYMAN, *Acta Cryst*. **B45** (1989) 218.
23. C. CLAUSEN, C. BAGGER, J. B. BILDE-SØRENSEN and A. HORSEWELL, *Solid State Ionics* **70/71** (1994) 59.
24. A. MITTERDORFER, M. CANTONI and L. J. GAUCKLER, in Proceedings of the Second European Solid Oxide Fuel Cell Forum, Oslo, May 1996, edited by B. Thorstensen, p. 373.
25. R. M. GERMAN and K. S. CHURN, *Metall. Trans. A* **15A** (1984) 747.
26. J. H. KUO, H. U. ANDERSON and D. M. SPARLIN, *J. Solid State Chem*. **83** (1989) 52.

Received 27 July
and accepted 26 August 1998